Rydberg electrons in laser fields: A finite-range-interaction problem

A. Giusti-Suzor
Laboratoire de Photophysique Moleculaire, Bâtiment 213, Université de Paris–Sud, 91406 Orsay, France

P. Zoller
Institute for Theoretical Physics, University of Innsbruck, A-6020 Innsbruck, Austria
(Received 11 May 1987)

A theory of Rydberg and continuum states in intense laser fields is developed based on the observation that the effect of laser radiation can be described in a scattering formulation as a finite-volume interaction coupling Coulomb-type fragmentation channels. In particular, laser-induced couplings may be incorporated in a multichannel quantum-defect treatment, in which a set of *dressed channels* corresponding to different photon numbers is defined, with *intensity-dependent* quantum defects and mixing angles. These quantities may be obtained by solving a system of close-coupling equations for the electron wave function, in a frame where the asymptotic electron oscillations are transformed away. This allows us to read off at a finite distance a radiative reaction matrix, which is a smooth function of energy for an energy range small compared with the photon frequency, and contains the net effect of radiative couplings. Calculations are presented for ionization of hydrogen s states in circularly polarized laser light, with allowance for above-threshold photon absorption.

I. INTRODUCTION

The development of powerful and tunable lasers has caused a rapid increase of multiphoton experiments, both in atoms and molecules. In these processes bound and autoionizing Rydberg states play an important role, as intermediate or final steps in the excitation sequence. Although Rydberg states have been widely studied in different contexts, the effect of an intense laser field on a Rydberg electron is seldom taken into account for the interpretation of the experimental spectra. Photoabsorption is usually treated at first nonvanishing order of perturbation theory, while it has been demonstrated that a strong field may affect much more deeply the dynamics of excited states.[1] In the high-energy parts of spectra, especially in the autoionization region of molecules, the large number of closely lying Rydberg levels and of ionization channels makes it necessary to define an efficient nonperturbative treatment of radiative coupling between several Rydberg series and continua.

On the other hand, theoretical work on laser-assisted electron collisions in the low-energy region, where a slow electron is scattered by an ionic target in presence of strong laser radiation, is presently in an initial stage.[2–4]

Obviously, the Rydberg and low-energy scattering problems are related, both involving threshold electrons moving mostly in a Coulomb field. This paper aims at emphasizing that they are actually identical, because the bulk of the field interaction, at least for uv or optical wavelengths, acts at short range, where the electron is strongly accelerated by the Coulomb forces and is insensitive to small differences in its asymptotic kinetic energy, either positive or negative. The short-range—or more generally finite-range—character of the electron-field interaction is physically grounded in the asymptotic behavior of the electron. At long range the effect of the time-dependent laser field amounts to elastic forced oscillations without real absorption or emission of photons, much as for a free electron ranging in a classical oscillating electric field. As will be shown below (Sec. II A), once in our theoretical treatment the asymptotic oscillations have been transformed away, the remaining interaction is a short-range potential coupling Coulomb channels.

The identification of radiative interaction as a short-range coupling opens the route for a theoretical approach which treats separately the short- and long-range processes and connects them in a further step. In particular, radiative couplings may be incorporated in a multichannel quantum-defect treatment (MQDT),[5–7] leading to the definition of a set of *dressed channels* with intensity-dependent phase shifts and mixing coefficients. These quantities may be obtained by perturbation theory for sufficiently weak fields or by solving, in a finite region of the space, a set of close-coupling equations which will be derived and discussed in Sec. II B. Specifying then the asymptotic behavior in each dressed channel (open or closed) will provide a unified description of an entire series of Rydberg states and the adjoining continuum in a laser field, and more generally of radiative coupling between several Rydberg series and continua. This approach, therefore, complements and extends the familiar two-level approach by making the wealth of MQDT concepts available to solve problems of the dressed atom in the field of quantum optics. The present treatment can be ranged among the nonperturbative methods for describing multiphoton ionization of atoms[8] or multiphoton dissociation of molecules.[9] This type of calculations, which have recently received a strong impulse due to the development of high-power lasers, includes all orders of interactions within a given set of Floquet channels[10] (or basis set), the accuracy being only limited by

the number of channels included.

As a first illustration, Sec. III describes the ionization process of Rydberg s states in an hydrogen atom, with allowance for above-threshold multiphoton absorption. The range of the radiative coupling, the number of partial waves to be included in the close-coupling system at a given laser intensity, and the energy dependence of the radiative reaction matrix are carefully discussed. Extensions to more complex cases are outlined.

II. SCHRÖDINGER EQUATION AND WAVE FUNCTION FOR ELECTRON IN LASER FIELD

A. The interaction Hamiltonian

We consider an electron moving in an atomic potential $V(\mathbf{x})$, which behaves asymptotically like a Coulomb potential, and under the influence of a (classical) laser field described by a vector potential $\mathbf{A}(\mathbf{x},t)$ in the Coulomb gauge. Its Schrödinger equation with the minimal coupling Hamiltonian, $H_V(t)$, for the wave function $\Psi_V(\mathbf{x},t)$ is

$$i\hbar\frac{\partial}{\partial t}\Psi_V(\mathbf{x},t)=\left[\frac{1}{2m}[\mathbf{p}-e\,\mathbf{A}(0,t)]^2+V(\mathbf{x})\right]\Psi_V(\mathbf{x},t)\ , \tag{2.1}$$

where $\mathbf{p}$ is the momentum operator. The subscript V for H_V and Ψ_V indicates that in first-order perturbation theory (in the light field) Eq. (2.1) leads to transition matrix elements in the velocity form. In Eq. (2.1) we have made the dipole approximation; this is valid to the extent we are able to restrict our considerations to an interaction volume small compared with the optical wavelength, a point which for the optical range will be justified below.

It is well known that by the unitary (gauge) transformation

$$\Psi_L(\mathbf{x},t)=e^{-ie\mathbf{x}\cdot\mathbf{A}(0,t)/\hbar}\Psi_V(\mathbf{x},t)\ ,$$

the Schrödinger equation (2.1) is transformed to a form with dipole "length" Hamiltonian, denoted by $H_L(t)$,

$$i\hbar\frac{\partial}{\partial t}\Psi_L(\mathbf{x},t)=\left[\frac{1}{2m}\mathbf{p}^2+V(\mathbf{x})-e\mathbf{x}\cdot\mathcal{E}(0,t)\right]\Psi_L(\mathbf{x},t)\ , \tag{2.2}$$

with $\mathcal{E}(0,t)=\mathcal{E}(t)\epsilon e^{-i\omega t}+\text{c.c.}=(\partial/\partial t)\,\mathbf{A}(0,t)$ the electric field at the position $\mathbf{x}=\mathbf{0}$. Here ϵ is the polarization vector, $\mathcal{E}(t)$ a slowly varying laser amplitude, and ω the laser frequency.

The same Schrödinger equation may still be written in a third form, obtained by transforming the wave function $\Psi_V(\mathbf{x},t)$ to a new frame, according to $\Psi_A(\mathbf{x},t)=e^{-\mathbf{p}\cdot\boldsymbol{\alpha}(t)/\hbar}\Psi_V(\mathbf{x},t)$ with $\boldsymbol{\alpha}(t)$ the solution of Newton's equation $m(d^2/dt^2)\boldsymbol{\alpha}(t)=e\mathcal{E}(0,t)$ for a free electron oscillating in the laser field. In this "space-translated frame"[11] the Schrödinger equation is

$$i\hbar\frac{\partial}{\partial t}\Psi_A(\mathbf{x},t)=\left[\frac{1}{2m}\mathbf{p}^2+V(\mathbf{x}+\boldsymbol{\alpha}(t))+\tfrac{1}{2}m\dot{\boldsymbol{\alpha}}(t)^2\right]\Psi_A(\mathbf{x},t)\ . \tag{2.3}$$

In the Hamiltonian H_A in Eq. (2.3) the first and second terms correspond to the kinetic energy and the potential in the new frame, while the last term is just the energy $\frac{1}{2}m\dot{\boldsymbol{\alpha}}(t)^2$ of oscillation of a free electron, a term which gives rise only to a time-dependent phase factor for the wave function $\Psi_A(\mathbf{x},t)$. In writing Eq. (2.3) we have tacitly assumed that $\mathbf{A}(0,t)$, $\boldsymbol{\alpha}(t)$, and $\dot{\boldsymbol{\alpha}}(t)$ are zero for times before the laser pulse reaches the atom, and the subscript A for the wave function refers to the acceleration form for first-order transition matrix elements.

In discussing the Schrödinger equations (2.1)–(2.3) we emphasize the following points.

(i) The Schrödinger equations (2.1)–(2.3) are related by (time-dependent) unitary transformations; therefore, they make identical physical predictions. Note, however, that operators which correspond to "true physical observables" (in the sense of Cohen-Tannoudji *et al.*[12]) will differ in all three cases: The kinetic momentum operator, for example, is $\boldsymbol{\pi}_V=\mathbf{p}-e\,\mathbf{A}(0,t)$, $\boldsymbol{\pi}_L=\mathbf{p}$, and $\boldsymbol{\pi}_A=\mathbf{p}+m\dot{\boldsymbol{\alpha}}(t)$ in the first, second, and third cases, respectively [with $\mathbf{p}=(\hbar/i)\nabla$ the canonical momentum operator].

(ii) Approximate methods for solving the Schrödinger equation in a time-dependent field are usually based on separating the Hamiltonian $H(t)$ into an unperturbed Hamiltonian $H_0=(1/2m)\mathbf{p}^2+V(\mathbf{x})$, and an interaction part $H_1(t)$. In the three cases (2.1) to (2.3) the interaction Hamiltonians have the form

$$H_{1V}(t)=-\frac{e}{m}\mathbf{p}\cdot\mathbf{A}(0,t)+\frac{1}{2m}\mathbf{A}(0,t)^2\ , \tag{2.4a}$$

$$H_{1L}(t)=-e\mathbf{x}\cdot\mathcal{E}(0,t)\ , \tag{2.4b}$$

and

$$H_{1A}(t)=V(\mathbf{x}+\boldsymbol{\alpha}(t))-V(\mathbf{x})+\tfrac{1}{2}m\dot{\boldsymbol{\alpha}}(t)^2\ , \tag{2.4c}$$

respectively. Note that in view of the different relationships between the (physical) kinetic momentum operator $\boldsymbol{\pi}$ and the canonical momentum $\mathbf{p}$, H_0 has an entirely different physical meaning in each case.

A central point we wish to emphasize is that the three interaction Hamiltonians (2.4a)–(2.4c) put the *weight of the interaction into different regions of space:* Close to the atomic core, it is preferable to work with the dipole interaction Hamiltonian $H_{1L}(t)=-e\mathbf{x}\cdot\mathbf{E}(0,t)$, which there becomes a perturbation (in the sense that $H_{1L}\to 0$ for $r=|\mathbf{x}|\to 0$).[13] On the other hand, $H_{1A}(t)$ goes to zero asymptotically as it behaves for large r as

$$H_{1A}(t)=e^2/4\pi\epsilon_0\boldsymbol{\alpha}(t)\cdot\mathbf{x}/r^3+\cdots\ , \tag{2.5}$$

i.e., like the potential of an oscillating dipole, and thus this form is the most convenient when dealing with electrons in extended Rydberg orbitals or in the continuum. In the present exploratory work the calculations will be

restricted to hydrogen and we shall use the Hamiltonian $H_{1A}(t)$ in whole space. For complex atoms or molecules, the electronic wave functions are difficult to determine accurately inside the core region and the use of $H_{1A}(t)$ which requires precise knowledge of the wave functions near the origin is dangerous. One should thus solve the Schrödinger equation using the length form $H_{1L}(t)$ in an inner region, and the acceleration form in an outer region to ensure convergence. The wave functions in both regions should then be connected by the time-dependent unitary transformation leading from the fixed to the space-translated frame. This procedure, reminiscent of (but not identical to) the frame-transformation technique[7] in MQDT, has already been used by Peach[14] and Seaton[15] in calculating radial dipole matrix elements: They performed the radial integration in the length form r up to a value $r=a$ and then switched to the acceleration form r^{-2}, thus introducing a *surface term* to be evaluated at $r=a$. Extension of these ideas to radiative close-coupling equations will be one of the future developments of this work.

We conclude this section by pointing out the physical picture which emerges from this discussion. The electronic motion is governed by different forces in different regions of configuration space: Close to the core the atomic forces dominate; in the asymptotic domain the electron vibrates rapidly in the time-dependent optical laser field while the weak atomic force is responsible for a slow mean motion of the electron in the asymptotic Coulomb potential. Transitions from Rydberg states to different bound or free orbits by absorption or induced emission of laser photons occur in the *transition zone* between the two regions which are dominated by different forces.

B. The radiative close-coupling equations

We proceed in our discussion by studying the electron wave function in the presence of a laser field. According to the above considerations, this is most conveniently done in the space-translated form of the Schrödinger equation (2.3). The essential steps are (i) derivation of a system of (time-independent) close-coupling equations using a Floquet (Fourier) and angular momentum decomposition of the electron wave function in the laser field, thus defining a set of reaction channels involving the laser photons; (ii) identification of the coupling between channels involving different photon numbers as a *finite-range interaction* between Coulomb type fragmentation channels; (iii) definition of a *reaction matrix* at the border of the interaction zone, which describes the absorption and emission of laser photons and is a slowly varying function of energy; (iv) specifying the asymptotic conditions in each channel (open or closed), according to the methods of quantum-defect theory, to study the properties of Rydberg and continuum states in a laser field.

To be specific, we study in the following the simplest possible system, namely, a Rydberg electron in a hydrogen atom under the influence of circularly polarized light $\mathcal{E}(0,t)=\mathcal{E}_0\epsilon e^{-i\omega t}+\text{c.c.}$ $[\epsilon=-(\mathbf{e}_1+i\mathbf{e}_2)/\sqrt{2}]$ which is adiabatically turned on and off. The potential $V(\mathbf{x}+\boldsymbol{\alpha}(t))$ is now a Coulomb potential which is moving with angular frequency ω on a circle in the xy plane of our coordinate system. We have $\boldsymbol{\alpha}(t)=-\alpha_0[\mathbf{e}_1\cos(\omega t+\delta)+\mathbf{e}_2\sin(\omega t+\delta)]$ with the radius $\alpha_0(\geq 0)$ and phase δ defined by $-\sqrt{2}e\mathcal{E}_0/m\omega^2=\alpha_0 e^{-i\delta}$. In this case the Floquet ansatz

$$\Psi_A(\mathbf{x},t)=\sum_{N=-\infty}^{\infty}\sum_{l,m}F_{lm}^{(N)}(r)/rY_{lm}(\theta,\Phi)\times e^{-iN(\omega t+\delta)-iEt/\hbar}, \tag{2.6}$$

with $F_{lm}^{(N)}(r)$ a radial wave function and E a quasienergy, reduces the time-dependent Schrödinger equation (2.3) to a system of time-independent close-coupling equations,

$$\left[E+N\hbar\omega-\tfrac{1}{2}m\omega^2\alpha_0^2+\frac{\hbar^2}{2\mu}\left[\frac{d^2}{dr^2}-\frac{l(l+1)}{r^2}\right]-V_{lm,lm}^{(0)}(\alpha_0,r)\right]F_{lm}^{(N)}(r)-\sum_{N',l',m'}{}'V_{lm,l'm'}^{(N-N')}(\alpha_0,r)F_{l'm'}^{(N')}(r)=0\ . \tag{2.7}$$

Here the potential terms $V_{lm,l'm'}^{(N-N')}(\alpha_0,r)$ are defined as the Fourier coefficients of matrix elements of the potential $V(\mathbf{x}+\boldsymbol{\alpha}(t))$ between spherical harmonics function,

$$V_{lm,l'm'}^{(N-N')}(\alpha_0,r)=\frac{1}{2\pi}\int_0^{2\pi}d\psi\, e^{-i(N-N')\psi}\langle lm\mid V(\mathbf{x}+\alpha_0(\mathbf{e}_1\cos\psi+\mathbf{e}_2\sin\psi))\mid l'm'\rangle$$
$$=-\frac{e^2}{4\pi\epsilon_0}\sum_{k=|N-N'|}^{\infty}\langle lm\mid C_{k,N-N'}\mid l'm'\rangle(-1)^{N-N'}C_{k,-(N-N')}(\pi/2,0)r_<^k/r_>^{k+1}\ . \tag{2.8}$$

The second line in Eq. (2.8) has been derived with the help of the multipole expansion formula for Coulomb potentials with $C_{k,q}(\theta,\Phi)$ unnormalized spherical harmonics and $r_<=\min(\alpha_0,r)$, $r_>=\max(\alpha_0,r)$. The parameter α_0 plays the role of an intensity parameter in our problem. When the close-coupling equations (2.7) are rewritten in atomic units, the dimensionless parameter which determines the coupling between the channels in Eq. (2.7) is

$$\bar{\alpha}_0=\alpha_0/a_0=\sqrt{2}(2\ \text{Ry}/\hbar\omega)^2(I/I_0)^{1/2}\ , \tag{2.9}$$

with a_0 the Bohr radius, Ry the Rydberg unit, $I=2c\epsilon_0|\mathcal{E}_0|^2$ the light intensity, and $I_0=2c\epsilon_0\mathcal{E}_{\text{a.u.}}^2=1.4\times10^{17}$ W/cm^2 the atomic unit light intensity. In the close-coupling equations (2.7) each channel is

identified by the parameters $\{N,l,m\}$ with N the Floquet (photon) index and l,m angular momentum quantum numbers of the electron. The prime on the sum in Eq. (2.7) indicates that diagonal terms should be left out in performing the sum. Note that according to Eq. (2.8) channels $\{N,l,m\}$ with $N+l=$even (odd) are only coupled to channels $\{N',l',m'\}$ with $N'+l'=$even (odd).

The potential terms in Eq. (2.7) have the following properties. First of all, the potential $V^{(0)}_{lm,l'm}$ goes asymptotically like

$$V^{(0)}_{lm,l'm}(\alpha_0,r)=-\frac{e^2}{4\pi\epsilon_0}\left[\frac{1}{r}\delta_{ll'}-\frac{1}{2}\frac{\alpha_0^2}{r^3}\langle lm\mid C_{2,0}\mid l'm\rangle+\cdots\right]. \tag{2.10}$$

i.e., the leading diagonal term falls off like a Coulomb potential. Degenerate channels with different l and l' are coupled asymptotically by an $1/r^3$ potential. Equation (2.10) together with (2.7) identifies the thresholds of our system as $-N\hbar\omega+\frac{1}{2}m\omega^2\alpha_0^2$. In comparison with the zero-field value, the thresholds are shifted by $\frac{1}{2}m\omega^2\alpha_0^2=e^2\mid\mathcal{E}_0\mid^2/m\omega^2$, the oscillation energy of the free electron in a laser field. For the following it is convenient to rescale the energy E according to $E+\frac{1}{2}m\omega^2\alpha_0^2\rightarrow E$. The asymptotically dominant interchannel potential goes like

$$V^{(\pm1)}_{lm,l'm'}(\alpha_0,r)=\pm\frac{e^2}{4\pi\epsilon_0}\langle lm\mid C_{1,\pm1}\mid l'm'\rangle\frac{\alpha_0}{r^2}+\cdots, \tag{2.11}$$

which decays like $1/r^2$. It is essential that the interaction terms which asymptotically behave as $1/r^2$ couple only channels differing by one photon energy $\hbar\omega$, i.e., channels with different thresholds [see Eq. (2.11)].[16] Indeed, the asymptotic oscillations of the Coulomb functions in nondegenerate channels tend to interfere destructively, thus limiting the effective range of the coupling to a finite region. The border r_c of this region may be estimated from $r_c\gg r_s$ with r_s a stationary phase point defined by $\Delta k r_s\approx1$, where Δk is the difference between the local electron wave numbers belonging to channels differing by one photon energy $\hbar\omega$. A crude estimate shows that for energies near threshold this is equivalent to $r_s\approx\omega^{-2/3}$ (in atomic units), which shows that the interaction volume contracts with increasing frequency.[17] Note that $r_s\approx1/\Delta k\approx1/[dk/d\epsilon)\hbar\omega]$ with $dk/d\epsilon\approx\hbar v_{\mathrm{orb}(r)}$ corresponds to the distance where the local orbital frequency $\omega_{\mathrm{orb}}(r)=v_{\mathrm{orb}}(r)/r$ of the electron equals the laser frequency ω.[18] Quantitative results illustrating the finite size of the interaction volume will be presented in Sec. III A. Finally, we note that for optical transitions the radius r_c is much smaller than the laser wavelength. This implies the validity of the dipole approximation when calculating laser-induced Rydberg-continuum or free-free transitions.[19]

The above discussion has pointed out the role of the frequency in limiting the interaction volume. On the other hand, it is apparent from the form of the potential $V(\mathbf{x}+\boldsymbol{\alpha}(t))$ and its matrix elements (2.5) that the size of the interaction zone grows with the oscillation radius α_0. For the range of α_0 and ω values studied in Sec. III, we have $\alpha_0<r_s$, so that the frequency is the dominating factor to determine the boundary of the reaction zone.

The possibility of truncating the set of close-coupling equations (2.7) is mainly a question of light intensity for a given laser frequency. As we noted before, it is the dimensionless parameter $\bar{\alpha}_0$ which determines the strength of the coupling between the different fragmentation channels. For $\bar{\alpha}_0\ll1$ this coupling is weak and we expect the results of perturbation theory (with respect to the field intensity) to emerge in this limit. More specifically, we show in the Appendix that the close-coupling equations (2.7) reduce in the weak field limit to Dalgarno-Lewis-type equations,[20] which have been extensively used to perform the summations over the atomic spectrum in perturbative multiphoton calculations. On the other hand, for $\bar{\alpha}_0\geq1$ the interchannel coupling becomes strong and one expects that the size of the truncated system (the number of channels included) should be increased until convergence is found for the given light intensity. A discussion of convergence with increasing light intensity and comparison with perturbation theory results will be given in Sec. III for H in circularly polarized laser light.

C. The radiative reaction matrix

For a given energy E and N_{tot} channels included in the calculation, there are N_{tot} real independent solutions of the close-coupling system which may be written for $r>r_c$ as

$$F_{ij}(r)=s_i(r)\delta_{ij}+c_i(r)\mathcal{R}_{ij}\quad(r>r_c), \tag{2.12}$$

where $j=\{N_j,l_j,m_j\}$ denotes the index of the solution and i the channel components. $s_i=s(\epsilon_i,l_i,r)$ and $c_i=c(\epsilon_i,l_i,r)$ are energy-normalized regular and irregular Coulomb wave functions for the energy $\epsilon_i=E+N_i\hbar\omega$ [i.e., the electron energy referred to the threshold of channel i, dressed with N_i photons (see Fig. 3)]. $\mathcal{R}$ is a real symmetric matrix which varies slowly with the asymptotic electron energy since it is constructed at short range ($r\ll r_c$) where the electron is strongly accelerated by the Coulomb field.[21]

The physical interpretation of the smooth $\mathcal{R}$ matrix depends on the energy range considered. If all channels are open ($\epsilon_i>0$ for all i), $\mathcal{R}$ is the usual reaction matrix describing laser-induced transitions between alternative fragmentation channels (e.g., for inverse bremsstrahlung). The corresponding laser-assisted collision cross sections are obtained from the scattering matrix

$$\chi=(1+i\mathcal{R})(1-i\mathcal{R})^{-1}, \tag{2.13}$$

which is again a smooth function of energy E.

If only N_o channels are open, the $N_c=N_{\mathrm{tot}}-N_o$ closed channels ($\epsilon_i<0$) must be eliminated from the asymptotic wave function ($r\rightarrow\infty$) since the corresponding Coulomb functions s_i and c_i have exponentially

diverging components. This elimination leads to the MQDT expression of the effective reaction matrix R (dimensions $N_o \times N_o$), restricted to the open channel space,[5]

$$R = \mathcal{R}_{oo} - \mathcal{R}_{oc}[\tan(\pi\nu_c) + \mathcal{R}_{cc}]^{-1}\mathcal{R}_{co} , \quad (2.14)$$

with the subscripts o and c referring to a partitioning of $\mathcal{R}$ with respect to open and closed channels; $[\tan(\pi\nu_c)]_{ij} = \tan(\pi\nu_i)\delta_{ij}$ is an $N_c \times N_c$ diagonal matrix with ν_i effective quantum numbers defined by $\varepsilon_i = -1$ Ry$/\nu_i^2$. The analogous relation for the scattering matrix $S = (1+iR)/(1-iR)$ in terms of the smooth matrix χ is

$$S = \chi_{oo} - \chi_{oc}(e^{-2\pi i\nu_c} - \chi_{cc})^{-1}\chi_{co} . \quad (2.15)$$

Contrarily to $\mathcal{R}$ and χ, the matrices R and S vary rapidly with the energy (via the energy variables ν_i) in the vicinity of the complex poles of Eqs. (2.14) and (2.15), which correspond to Rydberg resonances in the closed channels. These resonances have a finite width due to the decay of the Rydberg electron into the ionization continuum. Explicit calculation of ionization rates of Rydberg states based on reaction or scattering matrix elements will be presented in Sec. III. Here we conclude by stressing that the weak energy dependence of the generalized reaction matrix $\mathcal{R}$, a central property due to the limited range of the radiative coupling, allows the system of coupled equations (2.7) to be solved on a broad energy grid. In particular, $\mathcal{R}$ can be extrapolated across a Rydberg threshold, thus describing simultaneously laser-induced continuum-continuum transitions and Rydberg-state properties. We will take advantage of this property in the calculations described below.

III. SOLUTION OF THE RADIATIVE CLOSE-COUPLING EQUATIONS FOR HYDROGEN

A. Range of the radiative coupling

The finite-range character of the radiative interaction is most easily discussed in the weak field limit $\bar{\alpha}_0 \ll 1$. The asymptotically dominating coupling between the fragmentation channels is the $\bar{\alpha}_0/r^2$ term (in a.u.). In first-order perturbation theory for a free-free transition $i = \{N=0, l, m\} \rightarrow j = \{N=\pm 1, l', m'\}$ we find the reaction matrix element

$$\mathcal{R}_{ij} = -\sqrt{2}\pi\bar{\alpha}_0 \langle l_i m_i | \boldsymbol{\epsilon}\cdot\mathbf{e}_r | l_j m_j \rangle \times \int_0^\infty dr\, s(\varepsilon_i, l_i, r) 1/r^2 s(\varepsilon_j, l_j, r) \quad (3.1)$$

(with s_i and s_j Coulomb functions normalized as in Ref. 5, r in a.u. and $\mathbf{e}_r$ a radial unit vector) which, of course, is proportional to the radial continuum-continuum transition matrix element in the acceleration form. Figure 1 is a plot of the accumulated radial integral as a function of the upper integration limit for $\varepsilon_i = 0$, $\varepsilon_j = \omega = 0.3$ Ry, and $l_i = 0,1,2$ ($l_j = l_i + 1$). The finite range of the radiative interaction is illustrated in Fig. 1 by the fact that the integrals have essentially converged in a region $r \leq 15a_0$. Note that the radial integrals are built at larger distances and decrease in magnitude for higher l values, due to the increasing centrifugal potential. This

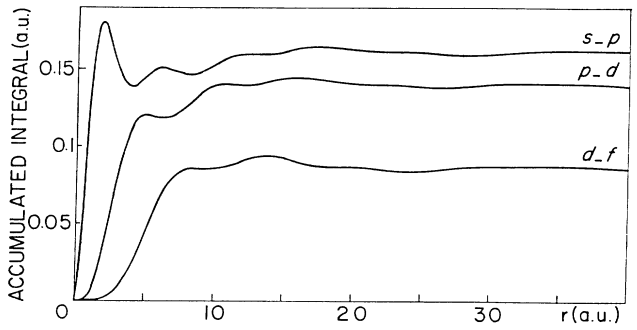

FIG. 1. Convergence of the radial integral in Eq. (3.1) for $l \rightarrow l+1$ dipolar transitions as a function of the upper integration limit r.

property is still more apparent on Fig. 2, where the radial matrix elements for $l \rightarrow l+1$ transitions are drawn as a function of l, for different photon energies: For a given frequency, the dipole moment becomes very small when the centrifugal barrier prevents the electron from penetrating into the core region. Another point which is clearly illustrated in Fig. 2 is the contraction of the interaction region with increasing photon frequency in accordance with the previous estimate $r_s \approx \omega^{-2/3}$: At high frequency, the magnitude of the transition matrix element drops much more rapidly when l increases. This property will help in restricting the number of partial waves to be included in the calculation, thus limiting the size of the close-coupling system.

It must be pointed out that the convergence with radial distance is slower for the matrix elements $\mathcal{R}_{ij}$ connecting two degenerate channels ($N_i = N_j$) for which interferences do not act destructively.[16] Nevertheless, these channels are coupled weakly by higher-order multipole terms [Eq. (2.10)], corresponding to indirect radiative transitions.

B. Solution of the close-coupling equations

To illustrate the method we have studied photoionization of *ns* Rydberg states of hydrogen by circularly polarized light as a function of light intensity. The discussion will be centered on the cases where single photoionization is energetically possible [$n > (1$ Ry$/\hbar\omega)^{1/2}$, see

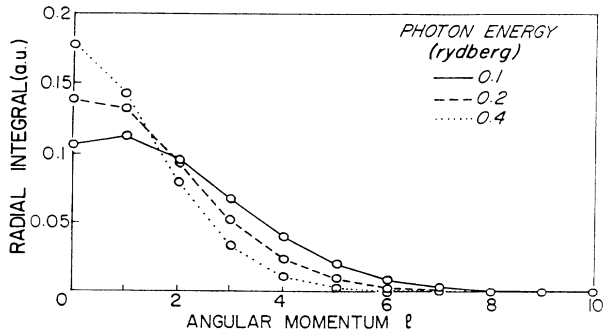

FIG. 2. Radial integral in Eq. (3.1) for $l \rightarrow l+1$ dipolar transitions as a function of l for different photon energies.

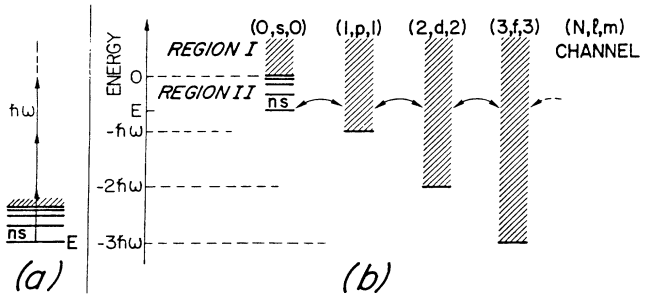

FIG. 3. Schematic representation of Rydberg-state multiphoton ionization in hydrogen. (a) Usual representation, (b) collisional (MQDT) representation; the arrows indicate the radiative transitions between the dressed channels. For simplicity stimulated emission is not indicated and only channels with $N=l$ are shown.

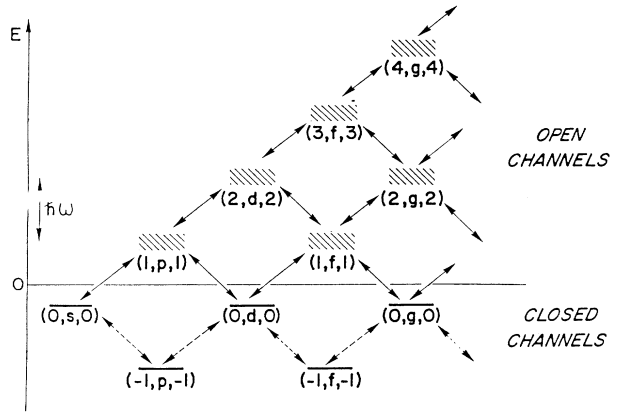

FIG. 4. Absorption and stimulated emission processes for an s electron in circularly polarized light. Only the processes involving up to five partial waves are indicated. Stimulated emission to the strongly closed channels (dashed arrows) is not included in the present work.

Fig. 3(a)], such that an increasing light intensity will cause absorption of additional photons in the continuum (above-threshold ionization). In its simplest form the system of close-coupling equations must include a single closed channel with an s electron and a number of open channels with higher l values [Fig. 3(b)]. At high intensities additional closed channels reached by stimulated emission must be introduced, as indicated in Fig. 4. In the present calculations we have included up to 25 channels with l values up to $l=8$, and Floquet indices $0\leq N\leq 8$.

The corresponding close-coupling system (2.7) is solved by propagating the solution typically out to $r_c\approx 50$ a.u. At r_c the channel radial wave functions are matched to pure Coulomb functions with corresponding l values and energies; the radiative reaction matrix is extracted according to Eq. (2.12). The calculations have been performed slightly above threshold [$E=0.01$ Ry, region I of Fig. 3(b)], but we have verified that almost identical results are obtained for energies just below threshold [$E<0$, region II of Fig. 3(b)]. More generally, the reaction matrix $\mathcal{R}$ is found to vary very slowly with energy, as expected for a given frequency ω (variations with ω are also smooth but much more noticeable).

An example of the convergence of the results with the size of the close-coupling system is given in Table I which shows values of the reaction matrix element $\mathcal{R}_{12}$ for various levels of truncation. We recall that the parameter $\bar{\alpha}_0$ [Eq. (2.9)] combines both the intensity and the frequency of the laser field. For the frequency $\omega=0.35$ Ry used in the calculations, perturbation theory—in which $\mathcal{R}_{12}$ is simply proportional to a dipole matrix element [Eq. (3.1)]—appears to be valid for intensities $I<10^{12}$ W/cm^2 ($\bar{\alpha}_0<0.1$). A satisfying convergence is reached in the nine-channel calculation ($0\leq N$, $l\leq 4$) for intensities of the order of 6×10^{13} W/cm^2 ($\bar{\alpha}_0\approx 1$), but up to 20 channels are needed in the intensity range 10^{14} W/cm^2.

At this stage of our calculations we have not included strongly closed channels corresponding to laser-induced transitions down to low-lying bound states (dashed arrows in Fig. 4, $N<0$). These states lead to the appearance of resonances; far away from these resonances one expects these deeply bound channels to make small contributions, but obviously they have to be included in further calculations. Having negligible amplitudes at the border r_c of the interaction region where the reaction matrix is extracted, these additional channels should not be treated as the other ones (open or weakly closed), but as "bound channels" (in the sense of Seaton in the Appendix of Ref. 5) eliminating their diverging components from the beginning. Inclusion of these strongly closed channels will induce a comparatively rapid variation with energy of the otherwise smooth reaction matrix $\mathcal{R}$ near the resonances, the low-lying bound states acting as isolated perturbers.[23]

TABLE I. Convergence of the reaction matrix element $\mathcal{R}_{12}$ with the size of the radiative close-coupling system. [−2] means $\times 10^{-2}$. $\omega=0.35$ Ry.

			Number of channels included[b]						
$\bar{\alpha}_0$	I (W/cm^2)	Perturb.[a]	4 ($l=2$)	6 ($l=3$)	9 ($l=4$)	12 ($l=5$)	16 ($l=6$)	20 ($l=7$)	25 ($l=8$)
0.1	6.6[11]	−4.37[−2]	−4.37[−2]	−4.37[−2]	−4.37[−2]				
0.5	1.6[13]	−2.18[−1]	−2.24[−1]	−2.26[−1]	−2.27[−1]	−2.27[−1]	−2.27[−1]		
1.0	6.6[13]	−4.37[−1]	−4.77[−1]	−4.95[−1]	−5.00[−1]	−5.01[−1]	−5.02[−1]	−5.02[−1]	−5.03[−1]
1.5	1.5[14]	−6.55[−1]	−8.40[−1]	−8.85[−1]	−9.05[−1]	−9.13[−1]	−9.16[−1]	−9.18[−1]	−9.20[−1]
2.0	2.6[14]	−0.87	−1.80	−1.82	−1.84	−1.85	−1.86	−1.86	−1.86

[a]Equation (3.1), $\mathcal{R}_{12}$ proportional to $\bar{\alpha}_0$.

[b]The l value in parentheses denotes the largest partial wave included in the calculation.

C. ac-Stark broadening and shift of *ns* Rydberg states

The ionization width and shift of the members of the *ns* Rydberg series are easily obtained from the smooth scattering matrix χ introduced in Sec. II C, more precisely, from the poles of the scattering matrix S defined by Eq. (2.15), i.e., the complex roots of the equation

$$\det(\chi_{cc}-e^{-2\pi i\nu_c})=0 \ . \tag{3.2}$$

In the present calculation all the closed channels have the same threshold energy (Floquet index $N=0$) such that $\nu_c=\nu=(-1\ \text{Ry}/E)^{1/2}$ is a scalar matrix. In this case (3.2) has solutions $\nu=n-\mu_\rho$ (n integer) where $\mu_\rho=\alpha_\rho+i\beta_\rho$ ($\rho=1,\ldots,N_c$) are complex quantum defects defined by

$$Z^{-1}\chi_{cc}Z=e^{2\pi i\mu_\rho} \ , \tag{3.3}$$

with Z a complex orthogonal matrix.[5,24] Thus we obtain for the complex energies

$$E^c_{n,\rho}=-1\ \text{Ry}/(n-\alpha_\rho-i\beta_\rho)^2=E_{n,\rho}-i\Gamma_{n,\rho}/2 \ , \tag{3.4}$$

whose real parts identify the resonance energies (including an ac-Stark shift) referred to the *shifted* $N=0$ threshold [compare Eq. (2.7) and following discussion], while the imaginary parts $\Gamma_{n,\rho}$ represent the full widths at half maximum of the resonances[25]

$$\begin{aligned} &E_{n,\rho}\approx-1\ \text{Ry}/(n-\alpha_\rho)^2\approx-1\ \text{Ry}/n^2-2\ \text{Ry}\alpha_\rho/n^3 \ , \\ &\Gamma_{n,\rho}\approx 2\ \text{Ry}\beta_\rho/(n-\alpha_\rho)^3 \ , \end{aligned} \tag{3.5}$$

provided one has $\beta_\rho \ll n-\alpha_\rho$, which is always the case in the range of intensities considered. Note that the Stark shift represented by α_ρ does not contain the contribution of low-lying bound states since our calculation does not include channels with $N<0$.

Equation (3.5) shows that both the shift and the width scale roughly as n^{-3} for a given series. The new feature, when compared with the usual MQDT applications, is that the complex quantum defects μ_ρ are intensity dependent. At moderate intensities ($\bar{\alpha}_0 \ll 1$) the coupling between the closed channels $l=0,2,4,\ldots$ is weak and the matrix χ_{cc} is almost diagonal (Z is almost a unit matrix). In this case the dressed channels may be approximately identified with the bare channels and the $\beta_1/(n-\alpha_1)^3$, $\beta_2/(n-\alpha_2)^3,\ldots$ are proportional to the ionization widths of the *ns*, *nd* states, etc. As an example, Fig. 5 shows the variation of β_1 as a function of the parameter $\bar{\alpha}_0^2$ [Eq. (2.9)]. The comparison between the results of several calculations, differing by the size of the close-coupling system, illustrates the need for increasing the number of channels (partial waves and Floquet blocks) at high intensities.

In order to visualize the behavior of these Rydberg levels with increasing laser intensity, Fig. 6 shows a model calculation of a resonantly enhanced multiphoton ionization spectrum which could be obtained by scanning the energy region just below threshold with a weak laser selectively exciting *ns* states. Ionization by this first weak probe laser is assumed to be negligible but a single photon absorption from a second intense laser is

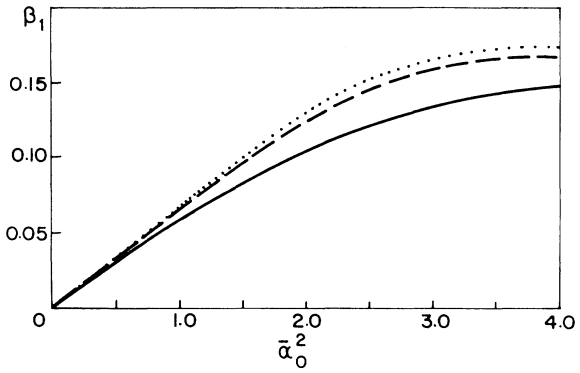

FIG. 5. Variation of the imaginary part of the complex quantum defect μ_1 [Eq. (3.3)] as a function of the intensity parameter $\bar{\alpha}_0^2$ [solid curve; 4-channel calculation ($0\le N,\ l\le 2$); dashed curve; 9-channel calculation ($0\le N,\ l\le 4$); dotted curve; 20-channel calculation ($0\le N,\ l\le 7$)]. The frequency is $\omega=0.35$ Ry.

able to ionize the resonant *ns* levels. The weak excitation process may be schematically described by a set of real dipole transition moments D_i (Ref. 5) associated with the set of channels of our MQDT treatment (dressed by the photons of the strong second laser). Assuming for simplicity that only the first closed channel ($N=l=m=0$) is excited ($D_i \propto \delta_{i1}$), an expression similar to Eq. (2.15) may be derived for the outgoing amplitudes in the open channels which in matrix notation reads[24]

$$\mathcal{D}=\mathcal{D}_o+\chi_{oc}Z(e^{2\pi i\mu_c}-e^{-2\pi i\nu_c})^{-1}Z^T\mathcal{D}_c \ , \tag{3.6}$$

where the $\mathcal{D}$'s are complex dipole moments related to the real ones, D, by $\mathcal{D}=-i/2(1+\chi)D$. Equation (3.6) leads to the partial cross sections (recall $D_i \propto \delta_{i1}$)

$$\sigma_i \propto |\mathcal{D}_i|^2 \tag{3.7}$$

for each open channel i, and to the total cross section σ_{tot} which is obtained by summing over the open channels. The ratio $\sigma_i/\sigma_{\text{tot}}$ calculated at the resonance ener-

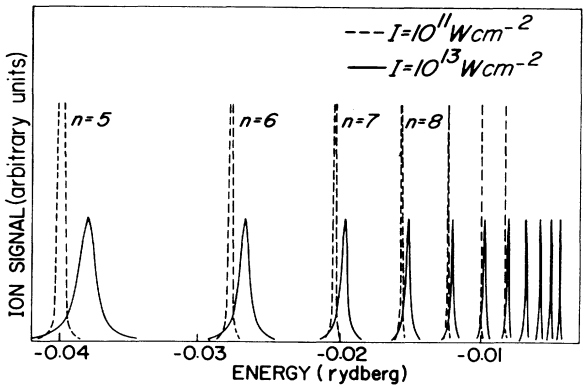

FIG. 6. Theoretical spectrum for the resonantly enhanced multiphoton ionization process of the *ns* Rydberg series in hydrogen for various laser intensities and circularly polarized light ($\omega=0.35$ Ry). Note that only the n-dependent part of the shift [Eq. (3.5)] is indicated.

gy E_{ns} [Eq. (3.5)] yields the branching ratio for ionization of the ns Rydberg state into the open channel i, i.e., after absorption of N_i photons. An explicit expression for the branching ratios in terms of the elements of the smooth χ matrix may be given in the simple case where only the first closed channel (ns Rydberg series) plays a role, i.e., at moderate intensity. Equations (3.6) and (3.7) then lead to the partial cross sections

$$\sigma_i \propto \cos^2(\pi\nu)\,|\chi_{i1}|^2/|e^{2\pi i\mu_1}-e^{-2\pi i\nu}|^2 \tag{3.8}$$

and to the total cross section

$$\sigma_{\rm tot} \propto \cos^2(\pi\nu)(1-|\chi_{11}|^2)/|e^{2\pi i\mu_1}-e^{-2\pi i\nu}|^2\,, \tag{3.9}$$

where the unitarity relation $\sum_i |\chi_{i1}|^2=1$ has been used. The branching ratios

$$\sigma_i/\sigma_{\rm tot}=|\chi_{i1}|^2/(1-|\chi_{11}|^2) \tag{3.10}$$

are energy independent in this case. In particular, they yield the partial ionization rates for the ns Rydberg states, which correspond as above to the poles in Eqs. (3.8) and (3.9). These poles cause the series of resonances in Fig. 6, where the total cross section (3.9) has been plotted in arbitrary units for different laser intensities. They have almost Lorentzian shapes due to our simplifying assumption of selective excitation of ns states in the closed channel, with a slight asymmetry due to the Stark shift and mixing with the continuum.

D. Multiphoton ionization rates

From the Stark broadening of the Rydberg states calculated in Sec. III C [Eq. (3.5)], one gets immediately the total ionization probability per unit time $\gamma_{ns}=\Gamma_{ns}/\hbar$. The partial ionization rates $\gamma_{ns}^{(k)}$ corresponding to the absorption of k photons is then obtained by multiplying the total ionization rates by the corresponding branching ratio.

The total and partial ionization probabilities of the $6s$ states are plotted in Fig. 7 as a function of the laser intensity for the frequency $\omega=0.35$ Ry. The straight lines correspond (in logarithmic coordinates) to perturbative results obtained in lowest order of perturbation theory for each partial rate $\gamma^{(k)}$ (proportional to I^k). The close-coupling values hardly depart from the perturbative ones below 10^{13} W/cm^2. A quantitative comparison

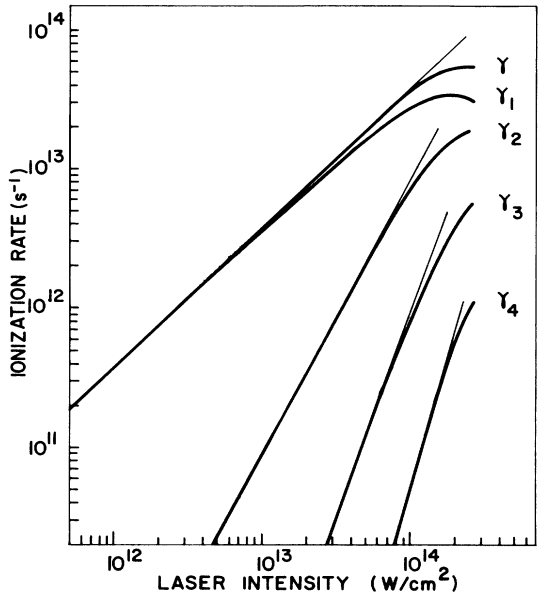

FIG. 7. Ionization rate of hydrogen $6s$ state by circularly polarized light ($\omega=0.35$ Ry). γ denotes the total ionization rate and $\gamma^{(k)}$ the partial rate for k-photon ionization.

with accurate perturbation calculations of above-threshold two-photon ionization[26,27] is given in Table II for some ns levels. The close-coupling equations have been solved slightly above threshold ($E=0.01$ Ry) at relatively weak intensities ($\bar{\alpha}_0=0.1$, see the second column) and for different frequencies as indicated in the first column. We have varied the radius r_c of the interaction zone (matching point to Coulomb functions) in order to demonstrate once again the finite-range character of the radiative interaction, since reasonable convergence is already obtained at $r_c=30$ a.u. The two-photon ionization rate for a given ns Rydberg state is simply obtained by multiplying the total rate (3.5) by the square of the corresponding χ matrix elements [Eq. (3.10)]. Note that the three n values for which comparison with previous perturbation results is possible at $\omega=0.2531$ Ry are obtained from a single close-coupling calculation and multiplication by a scaling factor n^{-3}. The agreement is very satisfying for the higher n values ($n=5,6$) and obviously becomes worse with decreasing n, since extrapo-

TABLE II. Two-photon ionization rates (10^9 s^{-1}) for ns Rydberg states of H in circularly polarized light. For a given frequency the close-coupling equations are solved at an energy $E=0.01$ Ry with four channels ($0\le N, l\le 2$), $\bar{\alpha}_0=0.1$, and different values r_c of the size of the reaction zone. In extrapolating to the bound-state region the energy dependence of the reaction matrix is ignored, i.e., the ionization rates for *all* ns states are obtained from a *single* calculation above threshold.

			Close-coupling calculations		Perturbation theory	
ω (Ry)	I (W/cm^2)	n	$r_c=30a_0$	$r_c=100a_0$	a	b
0.2531	1.79×10^{11}	6	0.285	0.282	0.285	0.286
		3	2.28	2.27	2.39	2.40
		2	7.70	7.66		9.12
0.3375	5.67×10^{11}	3	3.09	3.07	3.26	3.27
0.3645	7.72×10^{11}	5	0.721	0.717	0.732	0.734

[a]From Klarsfeld and Maquet (Ref. 26).
[b]From Aymar and Crance (Ref. 27).

lation below threshold of χ matrix elements without any energy dependence becomes less and less valid.

Above 10^{13} W/cm^2 ($\bar{\alpha}_0 > 0.5$) the partial rates for the lowest-order processes saturate (curves $\gamma^{(1)}$ and $\gamma^{(2)}$ on Fig. 7). From an analysis of our numerical results we infer that the total rate (uppermost straight line on Fig. 7) is slightly larger than the prediction of first-order perturbation theory (golden-rule result) in the intensity range below 5×10^{13} W/cm^2 and then becomes smaller. An important point to be noted is that the total ionization probability per unit time remains very close to the golden-rule result up to intensities for which the partial rates already differ notably from their lowest-order perturbation values. The large range of intensities for which the golden rule is valid for the total rate is somewhat surprising but has already been noted in experiments[28] as well as in calculations, e.g., by Crance and Sinzelle.[8] This results from a balance between the alternative ionization continua, the saturation of the lowest-order processes being partly compensated by the growth of higher-order processes. Above-threshold ionization tends to redistribute electrons among the available continua.

Finally, we give in Fig. 8 a schematic representation of the energy distribution of the photoelectrons[29] produced at the top of one of the *ns* resonances in Fig. 6, for various laser intensities: Additional peaks appear progressively when the laser intensity increases, and the relative weight of the first peak decreases. Note that the highest intensity (2.6×10^{14} W/cm^2) corresponds to a moderate value of the coupling parameter ($\bar{\alpha}_0=2$) due to the large value of the frequency ω. Comparison with experiments[30] and calculations extending to higher intensities in order to study the shape of the photoelectron spectrum are postponed to later publications.

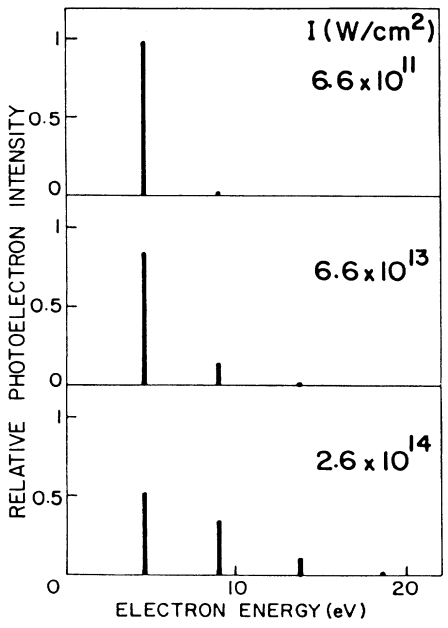

FIG. 8. Theoretical photoelectron energy distribution in the ionization process of hydrogen *ns* states for various laser intensities and circularly polarized light ($\omega=0.35$ Ry). The values of the coupling parameter $\bar{\alpha}_0$ are 0.1, 1, and 2, respectively (from top to bottom).

IV. CONCLUSIONS

The various results described in Sec. III have confirmed the finite-range character of the interaction between slow electrons in a Rydberg or continuum state and optical laser radiation. This property was predicted in Sec. II from the convergent character of the radiative Hamiltonian, expressed in a space-translated frame, and from destructive interferences between nondegenerate orbitals. The main consequence is the possibility of defining a radiative reaction matrix, which is slowly varying with energy, by solving a set of close-coupling equations on a finite range of radial distances. We have shown that convergence may be easily achieved both with respect to the border r_c of the interaction zone and the number of Floquet channels, for a given frequency and light intensity. Comparison with accurate perturbative results for two-photon ionization rates at low intensity demonstrate that a single calculation above threshold yields reasonable results for a large range of n states below threshold (at least $n \geq 5$). This point is encouraging for future development of our approach which is mainly intended as an efficient treatment of high Rydberg levels in complex multichannel situations, in the presence of a strong laser field.

The major development required for the handling of complex atoms and molecules is the implementation of a mixed gauge representation, combining the advantages of the length form at short distances and the acceleration form at large distances for the dipole radiative Hamiltonian. Then the radiative coupling could be treated in the inner zone on the same footing as the interelectronic interaction. Our approach will be particularly convenient for describing autoionizing states[31] due to the unified description of Rydberg and continuum states on one hand, and radiative and nonradiative interactions on the other hand. In the molecular case[32] a further advantage of the limited range of the radiative coupling is that calculations may be performed in the Born-Oppenheimer approximation framework (fixed internuclear distance and molecular symmetry) adapted to a Rydberg electron close to the molecular core. Perturbations and autoionizing processes due to rotations and vibrations can then be taken into account in a further step using the frame-transformation technique, which has been very successful in describing the low-intensity photoionization spectra.[33]

ACKNOWLEDGMENT

We thank Professor U. Fano for his strong interest in this work and continuous encouragement. We are also indebted to Dr. M. Crance whose comments have been very helpful for the completion of this work. One of us (P.Z.) acknowledges support by the Österreichische Fonds zur Förderung der wissenschaftlichen Forschung P6008P and Jubiläusmsfonds der Österreichischen Nationalbank under Project No. 2604.

APPENDIX: CONNECTION WITH PERTURBATION THEORY

In this appendix we establish the relationship between the familiar expressions for multiphoton transitions, obtained in lowest-order perturbation theory, and reaction matrix elements derived from the solution of the close-coupling equations (2.7) at low intensities. To be specific, we consider a two-photon process from an initial state (energy ε_i) with wave function $\langle \mathbf{x} \mid i \rangle = s(\varepsilon_i, l_i, r) Y_{l_i m_i}(\theta, \phi)$ to a final state with energy $\varepsilon_f = \varepsilon_i + 2\hbar\omega$ and wave function $\langle \mathbf{x} \mid f \rangle = s(\varepsilon_f, l_f, r) Y_{l_f m_f}(\theta, \phi)$. If we use as our starting point the dipole Hamiltonian $H_{1L}(t)$, we derive in second-order perturbation theory the transition matrix element

$$T_L^{(2)} = \langle f \mid (-e\mathbf{x}\cdot\boldsymbol{\epsilon}\mathcal{E}_0)(E_i + \hbar\omega - H_0 + i\epsilon)^{-1}(-e\mathbf{x}\cdot\boldsymbol{\epsilon}\mathcal{E}_0) \mid i \rangle \quad (\epsilon \to 0) \; . \tag{A1}$$

On the other hand, the interaction Hamiltonian $H_{1A}(t)$ leads to the expression

$$T_A^{(2)} = \langle f \mid [\alpha_{oc}\boldsymbol{\epsilon}\cdot\boldsymbol{\nabla}, V](E_i + \hbar\omega - H_0 + i\epsilon)^{-1}[\alpha_{oc}\boldsymbol{\epsilon}\cdot\boldsymbol{\nabla}, V] \mid i \rangle + \tfrac{1}{2}\langle f \mid [\alpha_{oc}\boldsymbol{\epsilon}\cdot\boldsymbol{\nabla}, [\alpha_{oc}\boldsymbol{\epsilon}\cdot\boldsymbol{\nabla}, V]] \mid i \rangle \tag{A2}$$

with the complex oscillation amplitude $\alpha_{oc} = -e\mathcal{E}_0/m\omega^2$. It is not difficult to prove that $T_L^{(2)} = T_A^{(2)}$ $(= T^{(2)})$ as expected from general considerations on gauge invariance.

In the Dalgarno-Lewis method[20] the calculation of the first term on the right-hand side of Eq. (A2) (which includes the infinite summation over the complete atomic spectrum) is reduced to solving an inhomogeneous differential equation. Defining

$$\mid \lambda \rangle = (E_i + \hbar\omega - H_0 + i\epsilon)^{-1}[\alpha_{oc}\boldsymbol{\epsilon}\cdot\boldsymbol{\nabla}, V] \mid i \rangle \; , \tag{A3}$$

we have to solve the set of equations

$$\begin{aligned} &(E_i - H_0) \mid i \rangle = 0 \; , \\ &(E_i + \hbar\omega - H_0) \mid \lambda \rangle = [\alpha_{oc}\boldsymbol{\epsilon}\cdot\boldsymbol{\nabla}, V] \mid i \rangle \; , \end{aligned} \tag{A4}$$

which—by comparison with Eq. (2.7)—reveals that (A4) can be identified as a truncated set of close-coupling equations where the term which couples the intermediate state $\mid \lambda \rangle$ *back* to $\mid i \rangle$ has been omitted.

The relation between the scattering matrix in second-order Born approximation, to be denoted by $\chi_{fi}^{(2)}$, and the transition matrix element $T_{fi}^{(2)}$ [Eq. (A2)] is easily established as $\chi_{fi}^{(2)} = -2\pi i T_{fi}^{(2)}$ for $\varepsilon_i > 0$. To the extent $\chi_{fi}^{(2)}$ is a smooth function it can be extrapolated to the bound region to give the ionization rate

$$W = \frac{2\pi}{\hbar} \mid T_{fi}^{(2)} \mid^2 \frac{dE}{d\nu}\bigg|_n = \frac{2\pi}{\hbar}\left|\frac{1}{2\pi i}\chi_{fi}^{(2)}\right|^2 \frac{dE}{d\nu}\bigg|_n \tag{A5}$$

for a Rydberg state with principal quantum numbers n. The factor $(dE/d\nu) \mid_n \approx \nu_n^{-3}$ converts from energy normalization to the usual normalization of the bound-state wave function to unity.

[1]See the various contributions in *Multiphoton Ionization of Atoms*, edited by S. L. Chin and P. Lambropoulos (Academic, New York, 1984).

[2]For reviews see L. Rosenberg, Adv. At. Mol. Phys. **18**, 1 (1982); F. Ehlotzky, Can. J. Phys. **63**, 907 (1985).

[3]M. Gavrila and J. Z. Kaminski, Phys. Rev. Lett. **52**, 613 (1984); in *Fundamentals of Laser Interactions*, Vol. 229 of *Lecture Notes in Physics*, edited by F. Ehlotzky (Springer, New York, 1985), p. 3.

[4]L. Dimou and F. H. M. Faisal, in *Photon and Continuum States of Atoms and Molecules*, Vol. 16 of *Springer Proceedings in Physics*, edited by N. K. Rahman, C. Guidotti, and M. Allegrini (Springer, Berlin, 1987).

[5]M. J. Seaton, Rep. Prog. Phys. **46**, 167 (1983).

[6]C. Greene and Ch. Jungen, Adv. At. Mol. Phys. **21**, 51 (1985).

[7]U. Fano and R. P. Rau, *Atomic Collisions and Spectra* (Academic, New York, 1986).

[8]Shih-I Chu and W. P. Reinhardt, Phys. Lett. **39**, 1195 (1977); Y. Gontier, N. K. Rahman, and M. Trahin, Phys. Rev. A **24**, 3102 (1981); Nuovo Cimento D **4**, 1 (1984); Shih-I Chu and J. Cooper, Phys. Rev. A **32**, 2769 (1985) and references cited therein; J. T. Broad, *ibid.* **31**, 1494 (1985); M. Crance and J. Sinzelle, in *Fundamentals of Laser Interactions*, Vol. 229 of *Lecture Notes in Physics*, edited by F. Ehlotzky (Springer, New York, 1985), p. 290.

[9]A. D. Bandrauk and M. L. Sink, J. Chem. Phys. **74**, 1110 (1981); Shih-I Chu, *ibid.* **75**, 2215 (1981); C. Leforestier and R. E. Wyatt, Phys. Rev. A **25**, 1250 (1982); F. H. Mies and P. Julienne, in *Spectral Lineshapes*, edited by F. Rostas (de Gruyter, Berlin, 1985), Vol. 3, p. 394.

[10]Shih-I Chu, Adv. At. Mol. Phys. **21**, 197 (1985).

[11]W. C. Henneberger, Phys. Rev. Lett. **21**, 838 (1968).

[12]C. Cohen-Tannoudji, B. Diu, and F. Laloe, *Quantum Mechanics* (Wiley, New York, 1977).

[13]When calculating dipole matrix elements, the contribution of the dipole length operator in the core region of (complex) atoms may even be neglected [Coulomb approximation; see D. R. Bates and A. Damgaard, Philos. Trans. R. Soc. London, Ser. A **242**, 101 (1949)].

[14]G. Peach, Mon. Not. R. Astron. Soc. **130**, 361 (1965).

[15]M. J. Seaton, J. Phys. B **14**, 3827 (1981); **19**, 2601 (1986); see also the mixed gauge representation of C. Chang and E. J. Robinson, *ibid.* **20**, 963 (1987).

[16]This asymptotic structure of the potential terms is in com-

plete analogy to what one finds in close-coupling equations for low-energy electron scattering from ions (with the exception of the hydrogenic $e + He^+$ problem, where the ion has degenerate energy levels which requires special considerations); see Ref. 5 and J. Dubau, J. Phys. B **11**, 4095 (1978).

[17]This contraction of the interaction zone with increasing frequency is consistent with the high-frequency approximation $\omega \to \infty$ for fixed α_0 described by Gavrila and co-workers (Ref. 3).

[18]U. Fano, Phys. Rev. A **32**, 617 (1985).

[19]Our conclusion is confirmed by the recent experiment by Leuchs *et al.* [G. Leuchs, S. Smith, S. Dixit, and P. Lambropoulos, Phys. Rev. Lett. **56**, 708 (1986)] who measured angular distributions in photoionization from Rydberg states. They found the quadrupole contributions to be much smaller than the dipole terms, with the ratio of quadrupole to dipole contributions being almost independent of the principal quantum number n (at least far away from bound-bound resonances).

[20]A. Dalgarno and J. T. Lewis, Proc. R. Soc. London, Ser. A **233**, 70 (1955).

[21]U. Fano, Phys. Rev. A **17**, 93 (1978); C. Greene, U. Fano, and G. Strinati, *ibid.* **19**, 1485 (1979).

[22]K. Rzazewski and R. Grobe, Phys. Rev. A **33**, 1855 (1986).

[23]For an example in the context of electron correlation, see M. Aymar, E. Luc-Koenig, and S. Watanabe, J. Phys. B **20**, 4325 (1987).

[24]J. Dubau and M. J. Seaton, J. Phys. B **17**, 381 (1984).

[25]A slightly different expression for the width of a Rydberg series of resonances, with $1/\pi \tanh(\pi\beta)$ instead of β in Eq. (3.5), has been given [A. Giusti-Szuzor and U. Fano, J. Phys. B **17**, 215 (1984) and Ref. 24]. For small values of β the two expressions yield identical results. With increasing β they start to depart from each other, but at the same time the concept of a width (which can be unambiguously assigned only to isolated resonances) breaks down.

[26]S. Klarsfeld and A. Maquet, Phys. Lett. **73A**, 100 (1979).

[27]M. Aymar and M. Crance, J. Phys. B **13**, L287 (1980).

[28]P. Kruit, J. Kimman, H. G. Muller, and M. J. Van der Wiel, Phys. Rev. A **28**, 248 (1983).

[29]S. I. Chu and W. Reinhardt, Phys. Rev. Lett. **39**, 1195 (1977); for a summary of work on above-threshold ionization (from atomic ground states) see the various contributions in Part II of *Photons and Continuum States of Atoms and Molecules,* Vol. 16 of *Springer Proceedings in Physics,* edited by N. K. Rahman, C. Guidotti, and M. Allegrini, (Springer, Berlin, 1987); Z. Deng and J. H. Eberly, J. Opt. Soc. Am. B **2**, 486 (1985). Direct comparison with the present work is not possible, however, since we consider ionization from Rydberg states and not from the atomic ground state.

[30]D. E. Kelleher, M. Ligare, and L. Brewer, Phys. Rev. A **31**, 2747 (1985); H. G. Muller, H. B. van Linden van den Heuvell, and M. J. van der Wiel, Phys. Rev. A **34**, 236 (1986).

[31]P. Lambropoulos and P. Zoller, Phys. Rev. A **24**, 379 (1981).

[32]C. Cornaggia, D. Normand, J. Morellec, G. Mainfray, and C. Manus, Phys. Rev. A **34**, 207 (1986); J. H. M. Bonnie, J. W. J. Verschuur, H. J. Hopman, and H. B. van Linden van den Heuvell, Chem. Phys. Lett. **130**, 43 (1986).

[33]U. Fano, Phys. Rev. A **2**, 353 (1970); C. Jungen and O. Atabek, J. Chem. Phys. **66**, 5584 (1977); Ch. Jungen and D. Dill, *ibid.* **73**, 3338 (1980).